Electronic Supplementary Material (ESI) for Dalton Transactions

Observation of divergent isotope effects as well as metal ion-modulated T_C and spin-canting nature in isostructural supramolecular magnets

Wen-Bo Pei,[†] Jian-Sheng Wu, [†] Xiao-Ming Ren, *[†‡] Zheng-Fang Tian[†] and Jingli Xie*[⊥]

† State Key Laboratory of Materials-Oriented Chemical Engineering and College of Science, Nanjing University of Technology, Nanjing 210009, P. R. China

‡ State Key Laboratory & Coordination Chemistry Institute, School of Chemistry and Chemical Engineering, Nanjing University, Nanjing 210093, P.R. China

[⊥] School of Chemistry, Monash University, Clayton, Victoria 3800, Australia

Tel.: +86-25-83587820

Fax: +86-25-83587820

E-mail: xmren@njut.edu.cn (XMR); jingli.xie@monash.edu (JLX)

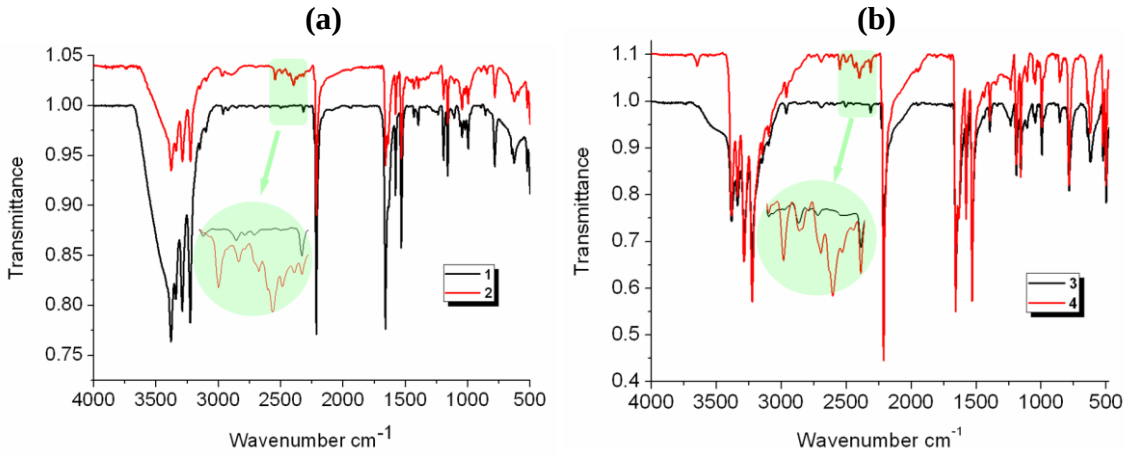

Figure S1 FT-IR spectra of (a) **1** and **2** (b) **3** and **4**. The spectroscopy changes owing to the deuteration in the region of 2320-2585 cm^{-1} showed inset.

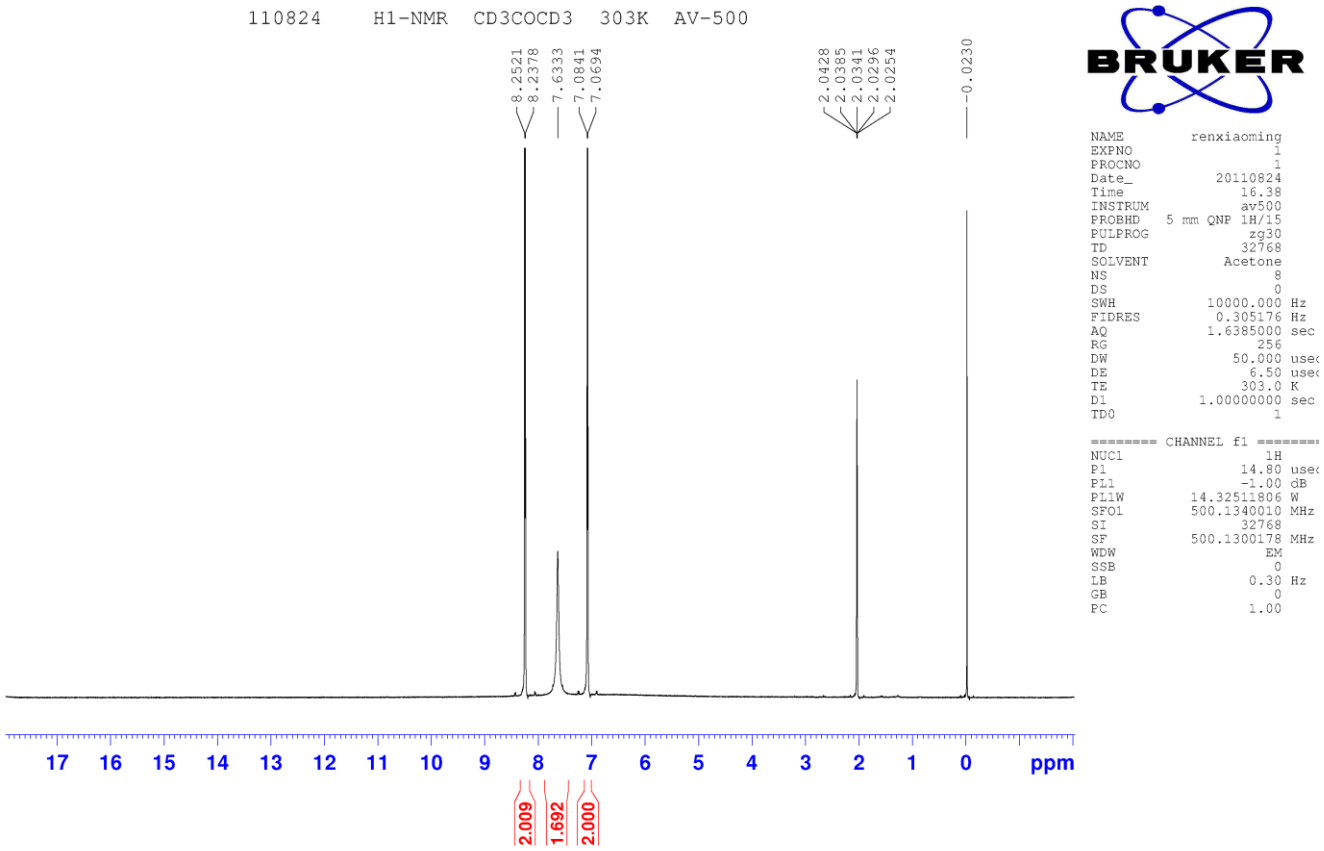

Figure S2 ^{1}H NMR spectra for [4-NH_2-PyD]$_2$[Pt(mnt)$_2$].

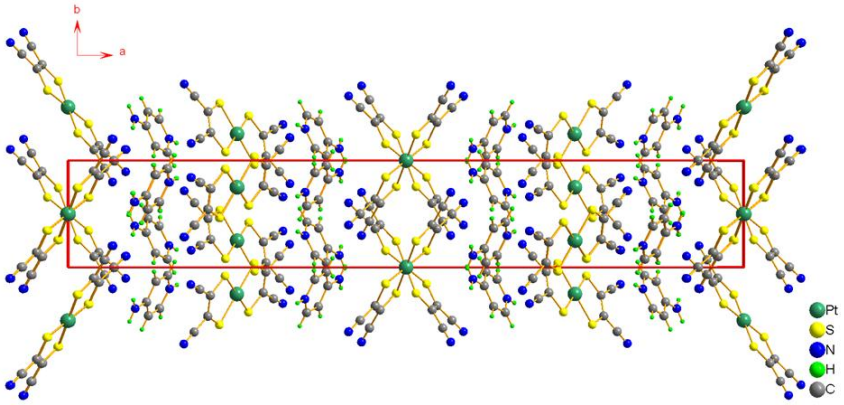

Figure S3 Packing diagram of **1** projected along *c*-axis, which shows the separated layered arrangements of both anions and cations

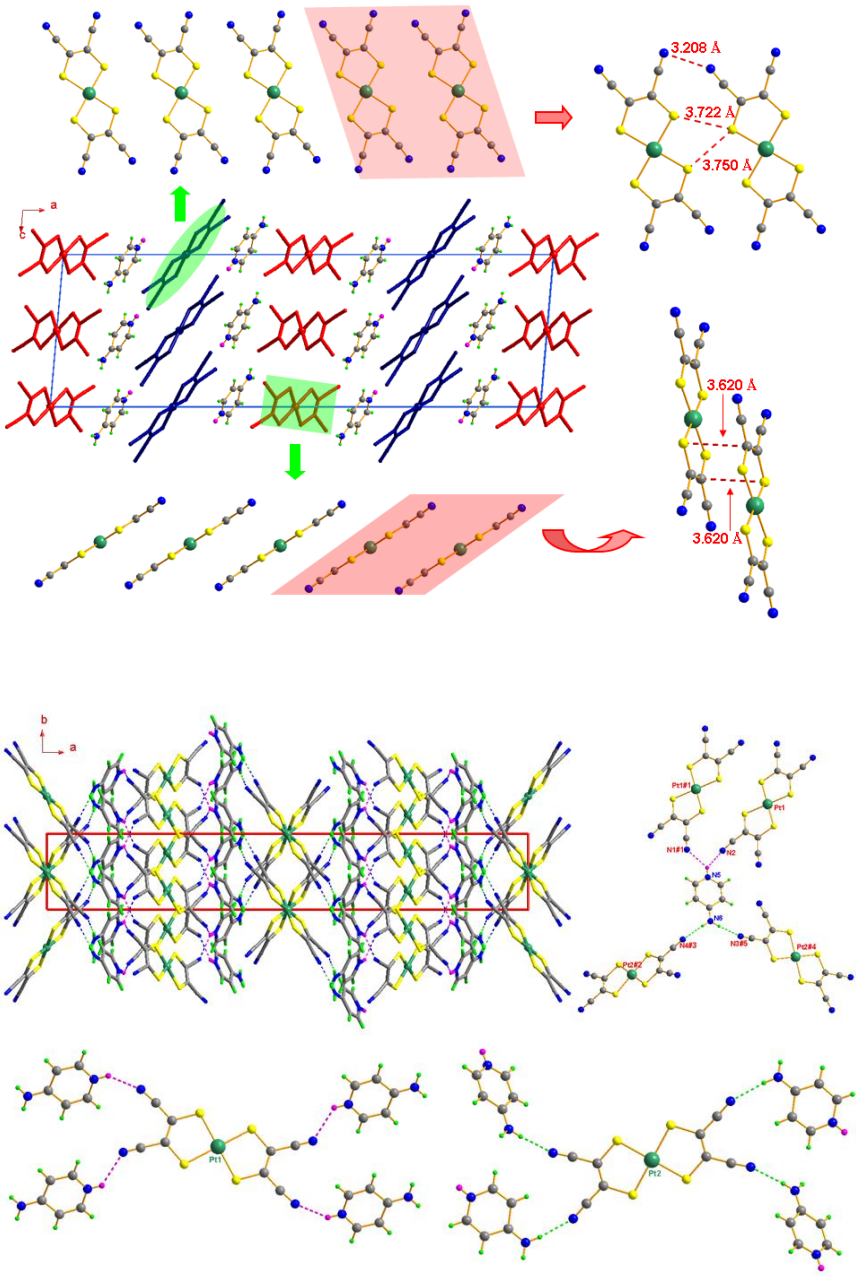

Figure S4 Packing diagrams of **2** projected along crystallographic *b*- and *c*-axes, respectively as well as hydrogen bond interactions between anions and cations (#1 = x, 1+y, z; #2 = -x, 1+y, 1.5-z; #3 = x, 2-y, 0.5+z; #4 = x, -1+y, z; # 5 = -x. –y, 1-z).

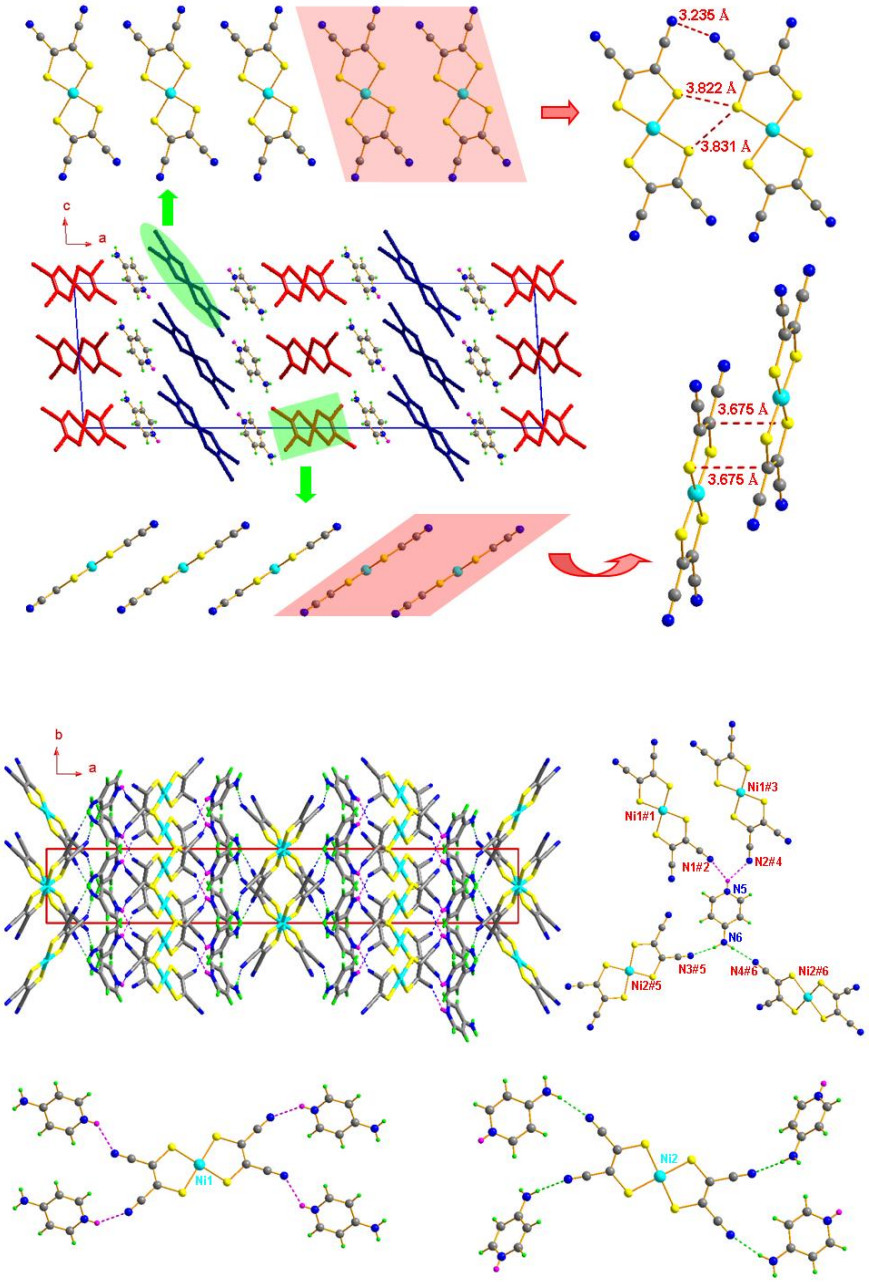

Figure S5 Packing diagrams of **4** projected along crystallographic *b*- and *c*-axes, respectively as well as hydrogen bond interactions between anions and cations (#1 = x, y, -1+z; #2 = 0.5-x, 0.5-y, -z; #3 = x, 1+y, -1+z; #4 = 0.5-x, 1.5-y, -z; #5 = -x, -1+y, 0.5-z; #6 = x, 1+y, z).

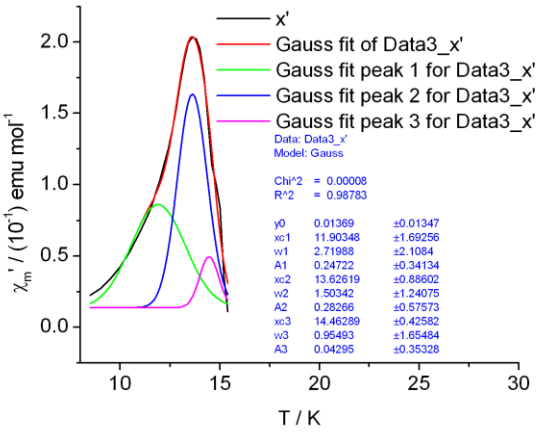

Figure S6 Three peaks with a Gaussian line shape were fitted using the fit-multi-peaks technique for the real part of the ac magnetic susceptibility of **2**, and the best fit gave three peak temperatures being 11.9, 13.6 and 14.5 K, respectively.

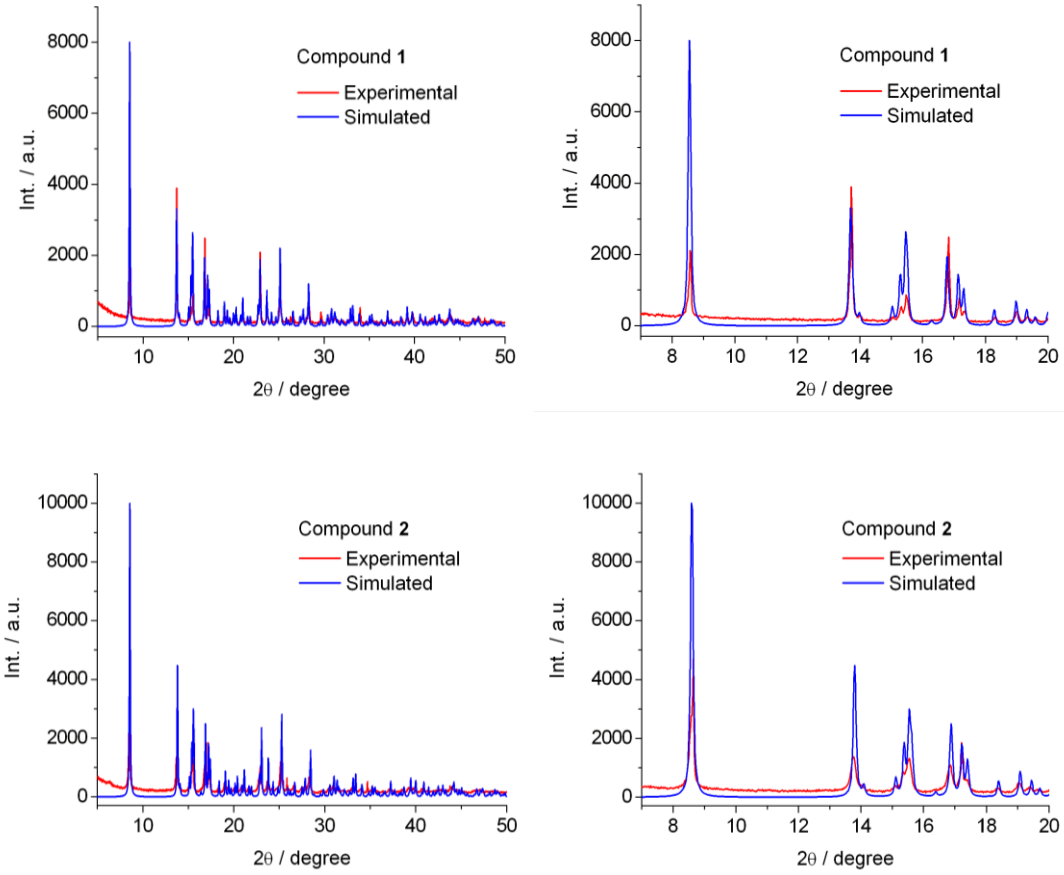

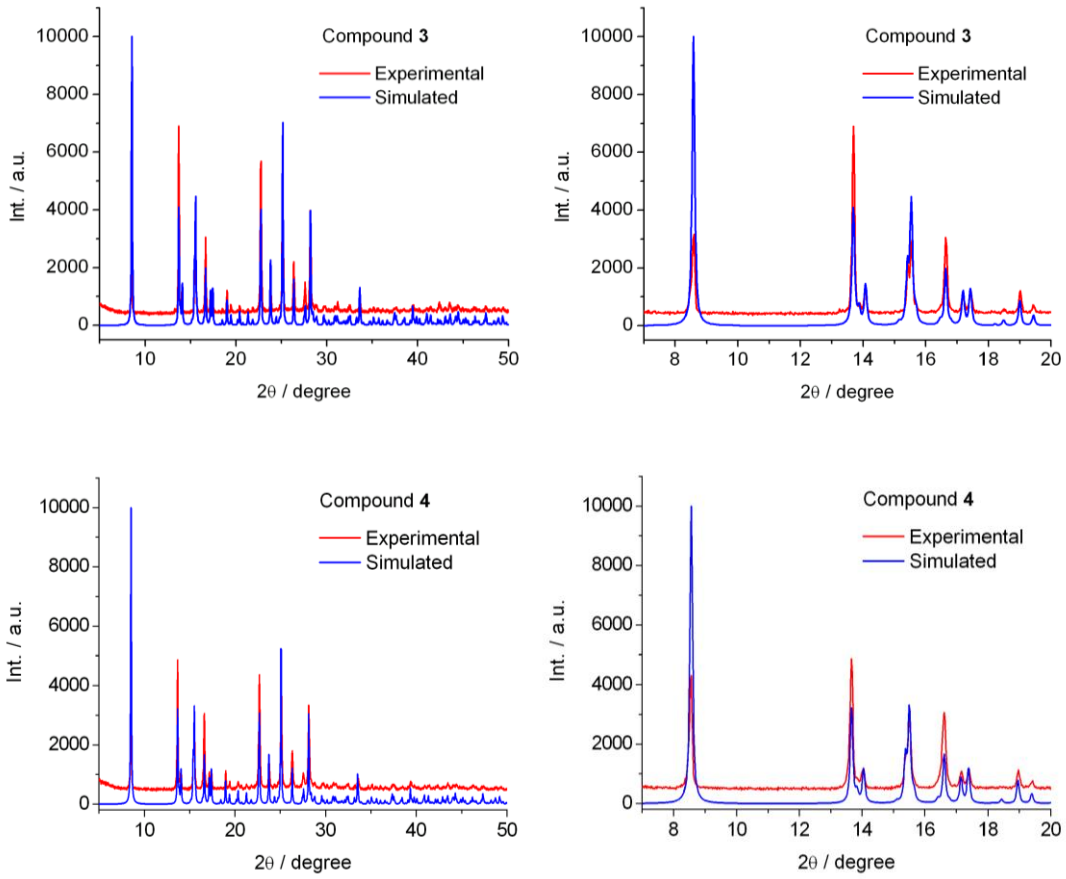

Figure S7 Powder X-ray diffraction patterns for **1**-**4** (red lines: experimental data; bluelines: simulation).

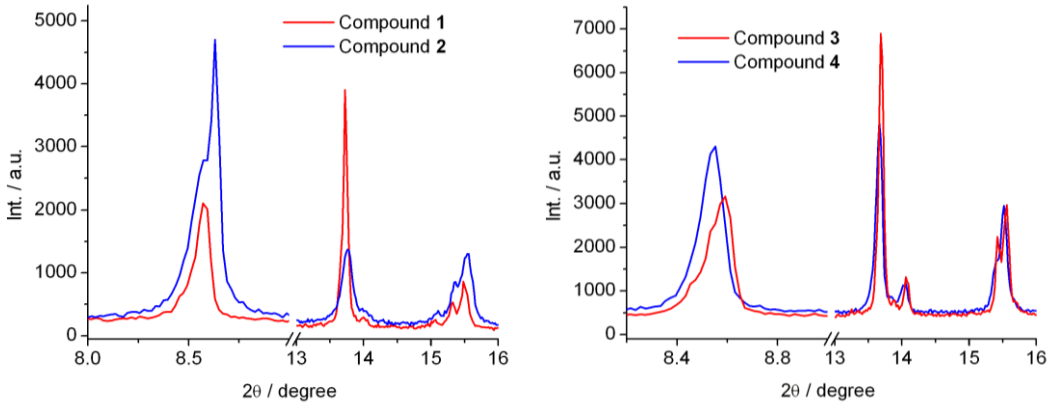

Figure S8 Comparison of powder X-ray diffraction patterns between **1** and **2** as well as between **3** and **4**.

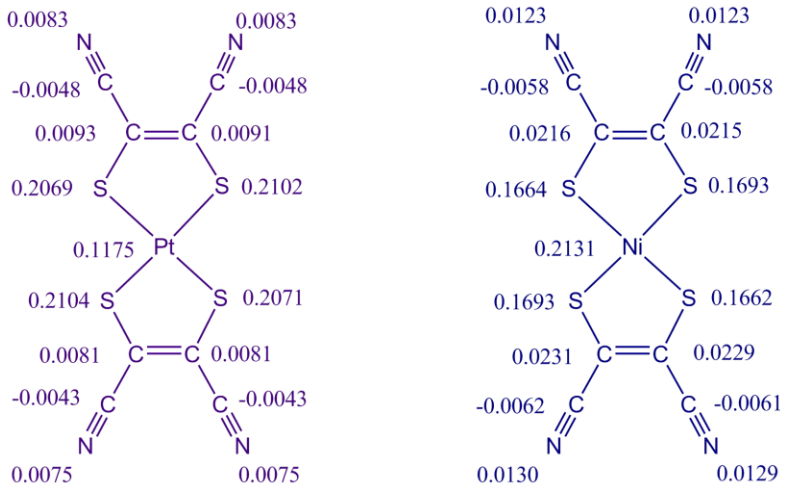

Figure S9 Spin density distributions of the Pt(2)-type $[Pt(mnt)_2]^-$ in **1** and Ni(2)-type $[Ni(mnt)_2]^-$ in **4**.